

Sublimation of Mars's southern seasonal CO₂ ice cap and the formation of spiders

Sylvain Piqueux, Shane Byrne, and Mark I. Richardson

Division of Geological and Planetary Sciences, California Institute of Technology, Pasadena, California, USA

Received 12 November 2002; revised 22 April 2003; accepted 6 May 2003; published 8 August 2003.

[1] In this paper we define and describe morphological features that have colloquially been termed “spiders” and map their distribution in the south polar region of Mars. We show that these features go through a distinct seasonal evolution, exhibiting dark plumes and associated fan-shaped deposits during the local defrosting of the seasonal cap. We have documented the seasonal evolution of the cryptic region and have found that spiders only occur within this terrain. These observations are consistent with a geyser-like model for spider formation. Association with the transparent (cryptic) portion of the seasonal cap is consistent with basal sublimation and the resulting venting of CO₂ gas. Also consistent with such venting is the observation of dark fan-shaped deposits apparently emanating from spider centers. Spiders are additionally confined to the polar layered deposits presumably due to the poorly consolidated and easily eroded nature of their upper surface. *INDEX TERMS*: 6225 Planetology: Solar System Objects: Mars; 5462 Planetology: Solid Surface Planets: Polar regions; 5415 Planetology: Solid Surface Planets: Erosion and weathering; 5470 Planetology: Solid Surface Planets: Surface materials and properties; 5464 Planetology: Solid Surface Planets: Remote sensing; *KEYWORDS*: Mars, spiders, geyser, polar, polar layered deposits, seasonal cap

Citation: Piqueux, S., S. Byrne, and M. I. Richardson, Sublimation of Mars's southern seasonal CO₂ ice cap and the formation of spiders, *J. Geophys. Res.*, 108(E8), 5084, doi:10.1029/2002JE002007, 2003.

1. Introduction

[2] The waxing and waning of the Martian seasonal ice caps has been observed for centuries [Kieffer *et al.*, 1992; James *et al.*, 1992]. Leighton and Murray [1966] suggested that these cycles represented the sublimation and condensation of CO₂, driven by seasonal variations in insolation. This cycle was first quantified with measurements of the surface pressure [Hess *et al.*, 1979], which varies annually with an amplitude of 25%. Since the CO₂ seasonal cap is in vapor equilibrium with the atmosphere, it responds immediately through sublimation and condensation to variations in absorbed insolation. The albedo of the seasonal ice is therefore a critical parameter, which in turn depends on the microphysical processes that are operating within the ice. An extreme example is the observed evolution of the “cryptic” region, primarily in the southern hemisphere [Kieffer *et al.*, 2000] but also recently recognized in the north [Kieffer and Titus, 2001]. These regions of the seasonal CO₂ ice caps exhibit low albedo, characteristic of the underlying regolith material, despite retention of substantial CO₂ ice covering, as evidenced by the observed brightness temperatures. It has been hypothesized that the simplest explanation for this “cryptic” terrain is the development in these regions of large-grained “slab” ice, which is transparent to visible light [Kieffer *et al.*, 2000]. Alternatively, these dark and

cold regions may be due to contamination of the seasonal ice with dust.

[3] Observations of the region surrounding the south polar cap from the Mars Orbiter Camera (MOC) show several unusual classes of geomorphic features. Among these are branching radial troughs emanating from central depressions. These features have been dubbed “spiders.” One hypothesis regarding the formation of these spiders is that they form through the channeling of CO₂ gas sublimed from beneath the transparent seasonal ice. This hypothesis [Kieffer, 2000] requires that solar radiation penetrate to the underlying regolith.

[4] In this study we test the hypothesis that the seasonal cap in the “cryptic” terrain sublimates from the bottom, forming jets, or “geysers,” of CO₂ gas that carve radial channels into the regolith surface (although this process is not identical to the geyser process on Earth, it is analogous, and so we use the term “geyser” throughout this paper). We do this by initially describing these spider features, which are observed in MOC images, and then by mapping their spatial distribution. We compare the mapped distribution against a “cryptic” region defined by albedo and surface brightness temperature maps from Thermal Emission Spectrometer (TES) data. The hypothesis that “spiders” are intrinsic signatures of a transparent slab ice process requires that spiders only form in cryptic terrain.

[5] In section 2 we describe spider features as observed in MOC imagery and describe our mapping approach and tools. These cases provide type members for our spatial mapping of spiders. In section 3 we present the results of

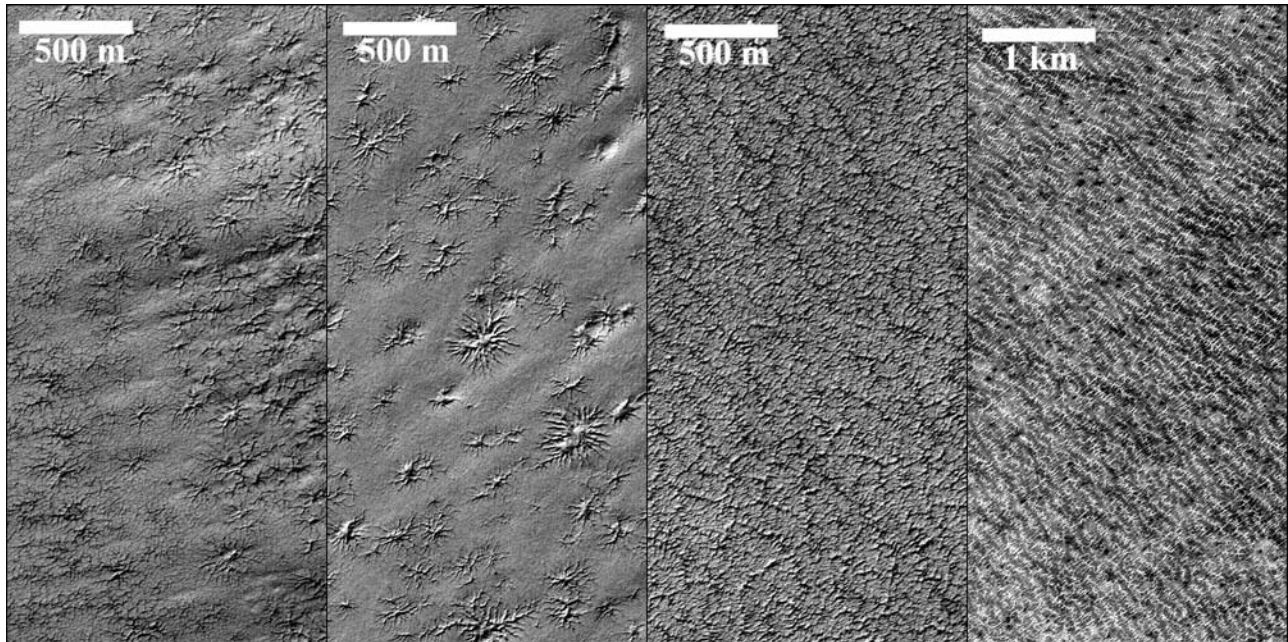


Figure 1. Examples of terrain which we have mapped as “spiders.” Both well-separated spiders (left two panels) and merged spiders (right two panels) were considered. The MOC narrow angle images are, from left to right, M11/02573 (87°S , 260°W , $L_s = 285^{\circ}$); M11/02368 (87°S , 233°W , $L_s = 284^{\circ}$); M11/03283 (87°S , 261°W , $L_s = 288^{\circ}$); and M09/00851 (87°S , 269°W , $L_s = 237^{\circ}$).

our mapping survey and describe their seasonal evolution in section 4. In section 5 we contrast them with definitions of the “cryptic” terrain based on TES albedo and thermal observations. In section 5 we also provide a complete mapping of the seasonal evolution of cryptic regional extent. Finally, in section 6 we provide a discussion of the observations within the context of a physical model for their formation.

2. Features, Data Sets, and Methodology

[6] The hypothesis to be tested in this paper suggests that sublimation of CO₂ occurs from the bottom of the seasonal ice cap in “cryptic” regions, generating “geyser flow channels” (or “spiders”) on the regolith surface underlying the cap. At a minimum the testing of this hypothesis requires demonstration that the “spiders” are associated with the “cryptic” region. As a result, this study requires a tool for collocating and simultaneously displaying data from multiple instruments aboard the Mars Global Surveyor (MGS): MOC, TES, and the Mars Orbiter Laser Altimeter (MOLA).

[7] In this study we make extensive use of a geographic information system (GIS) package, specifically customized by us for use in the Martian polar regions [Murray *et al.*, 2001; Byrne and Murray, 2002]. The specific GIS system employed is Arcview 3.2, made by the Environmental Systems Research Institute. The GIS system makes spatial relationships between imaging data sets clear by accurately and consistently projecting the data onto a common base map. Any data set that can be represented in a geographical image format can be projected in the GIS system, allowing the direct comparison of MOC, TES, and MOLA data products. In this study, MOC narrow angle (NA) images

and binned TES data products are overlain upon a 200 m pixel⁻¹ MOLA-derived digital elevation model. The MOC images were located relative to their surroundings using simultaneously acquired MOLA data, as described in more detail by Byrne and Murray [2002]. Over 5000 MOC narrow angle images were scrutinized for evidence of spider-like features.

[8] Figure 1 shows examples of radial structures observed in the southern polar latitudes with the MOC narrow angle camera. The term “spiders” was used by Kieffer [2000] (although the term may have originally been coined by Andy Ingersoll [H. Kieffer, personal communication, 2003]) and we use this term in this paper. The features displayed in Figure 1 are characteristic of what we have mapped throughout our region of interest. Spiders are typically characterized by a central depression with irregular troughs radiating away from the center. The spiders are shown to be “negative” features (depressions rather than knobs), based on illumination. These troughs merge and branch in an irregular and seemingly random pattern. Spiders occur only on the polar layered deposits; occurrences have been detected neither on the surrounding southern highlands nor on the southern residual cap. Spiders typically occur in groups, in some instances being packed densely enough to overlap. The central depressions are typically 50 m across; the entire spider, including its radial troughs, is typically 160–300 m across, although there are large variations.

[9] The area of our study was limited to regions poleward of 70°S and includes the southern residual cap, layered terrain (units Api and Apl [Tanaka and Scott, 1987; Kolb *et al.*, 2003]), and surrounding cratered and other units. Owing to constraints imposed by the spacecraft orbit, there is very little data in the area from 87°S latitude to the pole. This

area was therefore excluded from our study. We have mapped the location of the spiders by primarily using data from the mission phases M07–M11, corresponding to the period $L_s = 198^\circ$ – 290° (southern spring and summer, where L_s is the angular measure of season, measured in degrees from $L_s = 0^\circ$ at northern spring equinox). However, some data from all phases up to the end of E06 (July 2001, $L_s = 190^\circ$) were used when the lighting was good enough.

3. Distribution of Spiders

[10] The morphological definition of a spider as used in this study is described in section 2 and illustrated in Figure 1. The mapping of the spider distribution was undertaken, initially, without reference to the distribution of the cryptic terrain by systematically scrutinizing all MOC southern spring and summer NA images poleward of 70°S . Images containing spiders were labeled graphically by outlining the portion of a given image within which spiders were observed. These outlines were recorded within the GIS system.

[11] Figure 2a shows the distribution of spiders found in this study. The distribution is not spatially uniform. There is a considerable concentration of recorded spiders in the 180° – 270°W sector and poleward of 85°S . A generally elevated concentration exists poleward of 80°S from 130°W to 330°W , except near 82°S , 150°W , with other regions of concentration existing in this same longitude sector but farther equatorward. Within this region the spiders were found only on the surface of the layered deposits and not upon the surrounding basement. On the basis of their locations there appears to be no special elevation, slope, or surface roughness requirement for the formation of spiders. Very few spiders were found in the sector between 330°W and 360°W and 0° – 120°W . Those few found in this sector are located very close to the residual cap.

[12] In order to understand the significance of the observed spider distribution, it is necessary to examine the geographic distribution of available MOC NA images. Figure 2b shows the spatial distribution of MOC NA availability for all mission phases through E06. The MOC NA coverage is clearly not uniform, and a number of significant features in the MOC observational pattern can be discerned. There is a strong concentration of images on the outside edge of (and around) the so-called “polar” or “3°” ring, the area of very high repeat coverage associated with the 93° inclination of the MGS orbit. This ring is repeatedly imaged, generating multiple images of the same surface location over time, in order to study the seasonal and interannual variability of the surface. The residual cap is especially well covered where it falls on or equatorward of the 3° ring. There is also a strong concentration of images in the lower-latitude layered deposits between 180°W and 225°W and 72° – 78°S , resulting from observations taken initially to support and then to find the pulverized crash debris of the Mars Polar Lander (MPL). In particular, the MPL landing ellipse at 75° – 78°S and 190° – 195°W is intensely covered. Between 60°W and 90°W and poleward of 75°S an area of modest elevation of coverage is associated with Cavi Angusti, with a strong concentration on the “Inca city” at 81.5°S , 64°W . Figure 2b shows that we find spiders only in well-imaged areas of the layered deposits

and that substantial imaging coverage off the layered deposits revealed no spiders. As a result of this coverage analysis, we can state that the failure to observe significant numbers of spiders in the sectors 330° – 360°W and 0° – 120°W does not result from a lack of observations in that sector. Thus the longitudinal bias in spider occurrence evident in Figure 2a would appear to be real.

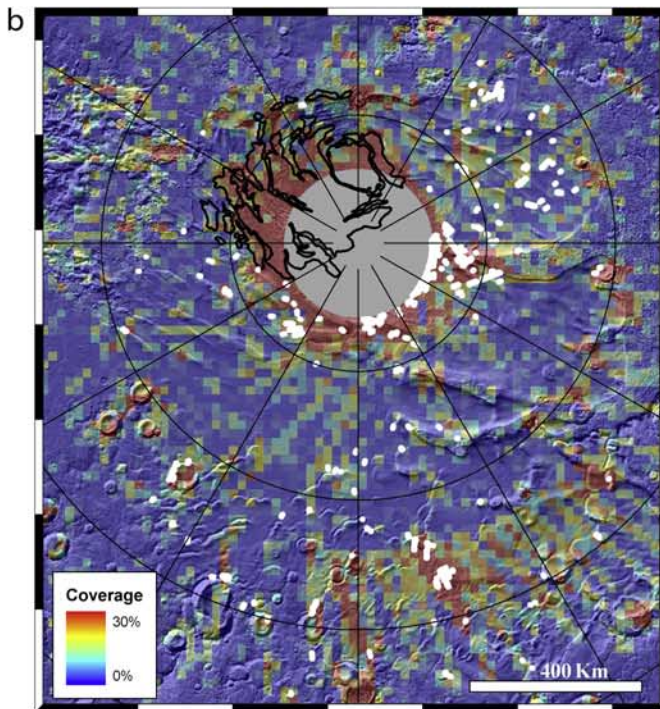
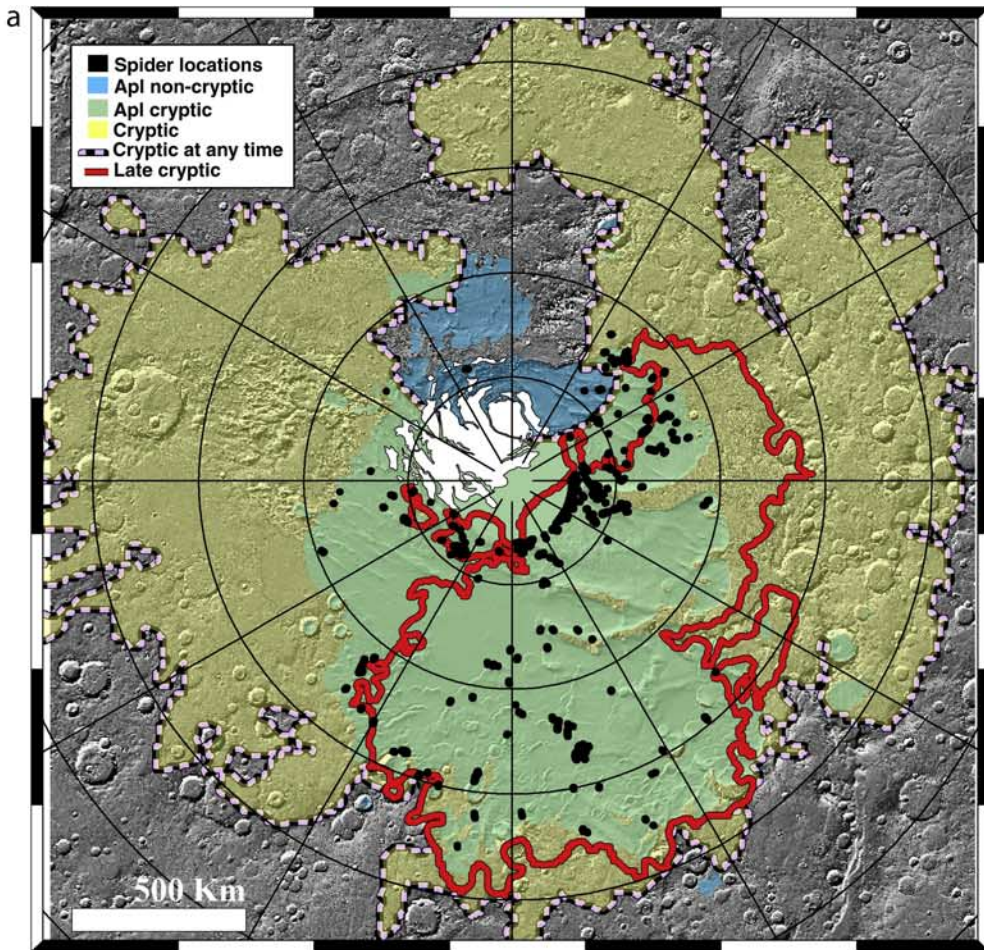
4. Seasonal Evolution of Spiders

[13] An example of the seasonal evolution of regions containing spiders is provided in Figure 3. The region shown in Figure 3 was repeatedly imaged (six times) by virtue of its location on the 3° ring, near the head of Chasma Australe on the layered deposits. Initially, at $L_s = 180^\circ$ the region is almost completely covered by bright seasonal frost (Figure 3a). Small dark spots indicate the position of spider features not yet visible, while brighter features in the image are primarily due to surface topography. By $L_s = 195^\circ$ (Figure 3b), the dark spots have expanded significantly, including the initial development of dark fans emanating from some of the spots. Figures 3c–3e show the gradual sublimation of the seasonal ice cap and the increasing visibility of spider structures. The fans increase in prominence in Figure 3c and develop clear directionality indicative of wind action. In Figures 3d and 3e the fans have developed into (or merged with or been replaced by) streaks that also show strong directionality, presumably associated with a somewhat different prevailing wind. As the seasonal ice cap diminishes, the spiders become bright relative to their surroundings. We interpret this to be due to (CO₂ or, more likely, water) frost being redeposited within the small-scale topography after the main seasonal cap has retreated. Figure 3f shows spiders as they appear during the summer (this image corresponds to $L_s = 275^\circ$). They are now distinguishable as topographic features rather than as albedo features.

[14] It should be noted that not all dark spots observed in early spring are associated with spider landforms. In this case they are not diagnostic of “geyser” processes. It seems likely to us that there are several different processes that can generate dark spots and streaks. For example, dark spots on sand dunes that develop due to differential sublimation may provide a source for saltating particles, which can spread over neighboring seasonal ice. However, a preponderance of dark spots and streaks on the cryptic terrain are associated with the appearance of spiders later in the season.

5. Relationship of Spiders to the Cryptic Terrain

[15] In order to test the CO₂ geyser hypothesis for the formation of spiders, we investigated the correlation between the regions within which spiders were identified and the regions of the southern seasonal ice cap that exhibit “cryptic” behavior. Cryptic terrain, as defined by Kieffer *et al.* [2000], is characterized by regions of low albedo within the southern seasonal cap that remain at the CO₂ sublimation temperature. The proposed explanation for this phenomenon is that the seasonal CO₂ ice cover forms a solid transparent slab, allowing the albedo of the underlying surface to show through but to keep its cold temperature.



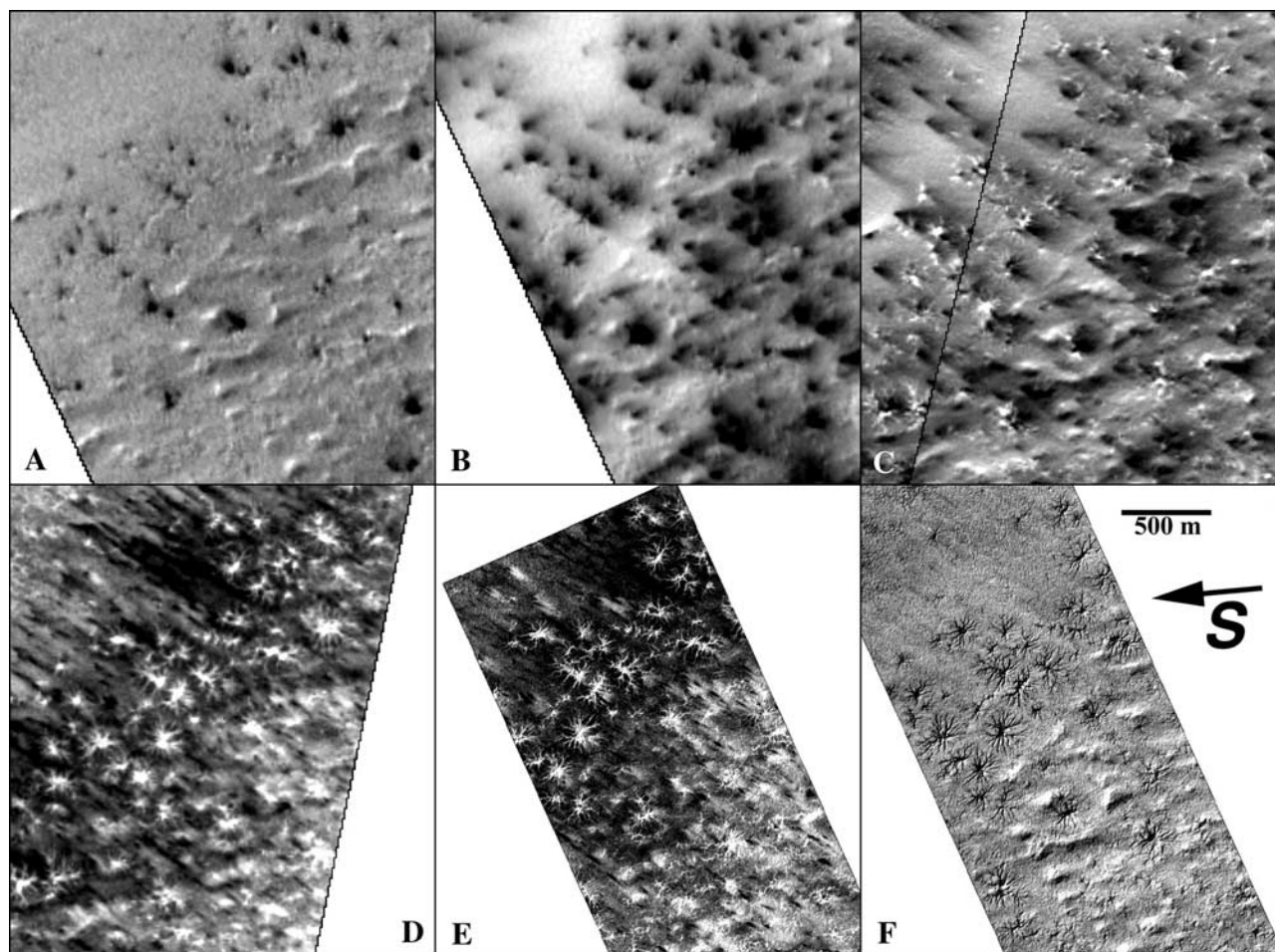


Figure 3. Comparison of the same area at 87°S, 275°W at different times during the Martian southern summer, illustrating the seasonal evolution in appearance that the spider features undergo. The MOC narrow angle images are (a) M03/05867 at $L_s = 180^\circ$; (b) M04/03488 at $L_s = 195^\circ$; (c) mosaic of M07/02549 and M07/05081 at $L_s = 208^\circ$ and 214° ; (d) M08/07709 at $L_s = 235^\circ$; (e) M09/00570 at $L_s = 237^\circ$; and (f) M11/00280 at $L_s = 275^\circ$. Each subframe has been independently stretched to bring out the maximum detail, so albedo is not directly comparable from subframe to subframe.

[16] In order to locate the boundary of the cryptic region, we have gridded data from the TES in intervals of 5° of solar longitude for both Lambert albedo and surface temperature (defined with the TES equivalent of the Viking T_{20} band). We delineated the extent of the cryptic region in a quantitative way by contouring the albedo data at a value of 0.38 for each interval of solar longitude. Only regions with albedos lower than this value and within the seasonal cap (which was determined using the surface temperature data)

were considered cryptic. The cryptic region evolves in shape as the seasonal cap recedes, as illustrated in Figure 4. The data shown in Figure 4 are derived from the first MGS mapping year and thus provide much more complete coverage and higher spatial and temporal resolution than the premapping data presented by Kieffer *et al.* [2000]. Initially, at $L_s = 175^\circ$ the cryptic region covers almost the full range of longitudes surrounding the residual cap. As the season progresses, the area designated as cryptic rapidly

Figure 2. (opposite) (a) The relationship between the distribution of spiders (black circles), two aggregate definitions of the cryptic terrain (dashed and solid lines), and the outline of the layered deposits [Kolb *et al.*, 2003] (blue or green shaded areas). The dashed line encloses all regions that exhibited cryptic behavior at any point between $L_s = 180^\circ$ and $L_s = 250^\circ$. The red solid line delineates the more consistently cryptic terrain from $L_s = 190^\circ$ onward. In this and subsequent map views the projection is polar stereographic; plotted latitude and longitude lines are every 5° and 30° , respectively (0° longitude is straight up). The residual CO₂ cap is shown in solid white. Background shading is provided by MOLA-derived shaded relief. (b) Illustration of MOC NA coverage in the south polar region. Coverage is defined as the percentage of terrain imaged at least once within a given area. The residual cap outline is shown in black, and the distribution of spider landforms is shown as white spots. Latitude and longitude lines are every 5° and 30° , respectively. Although the scale is maximized at 30%, many areas, such as the polar ring, have $>90\%$ coverage.

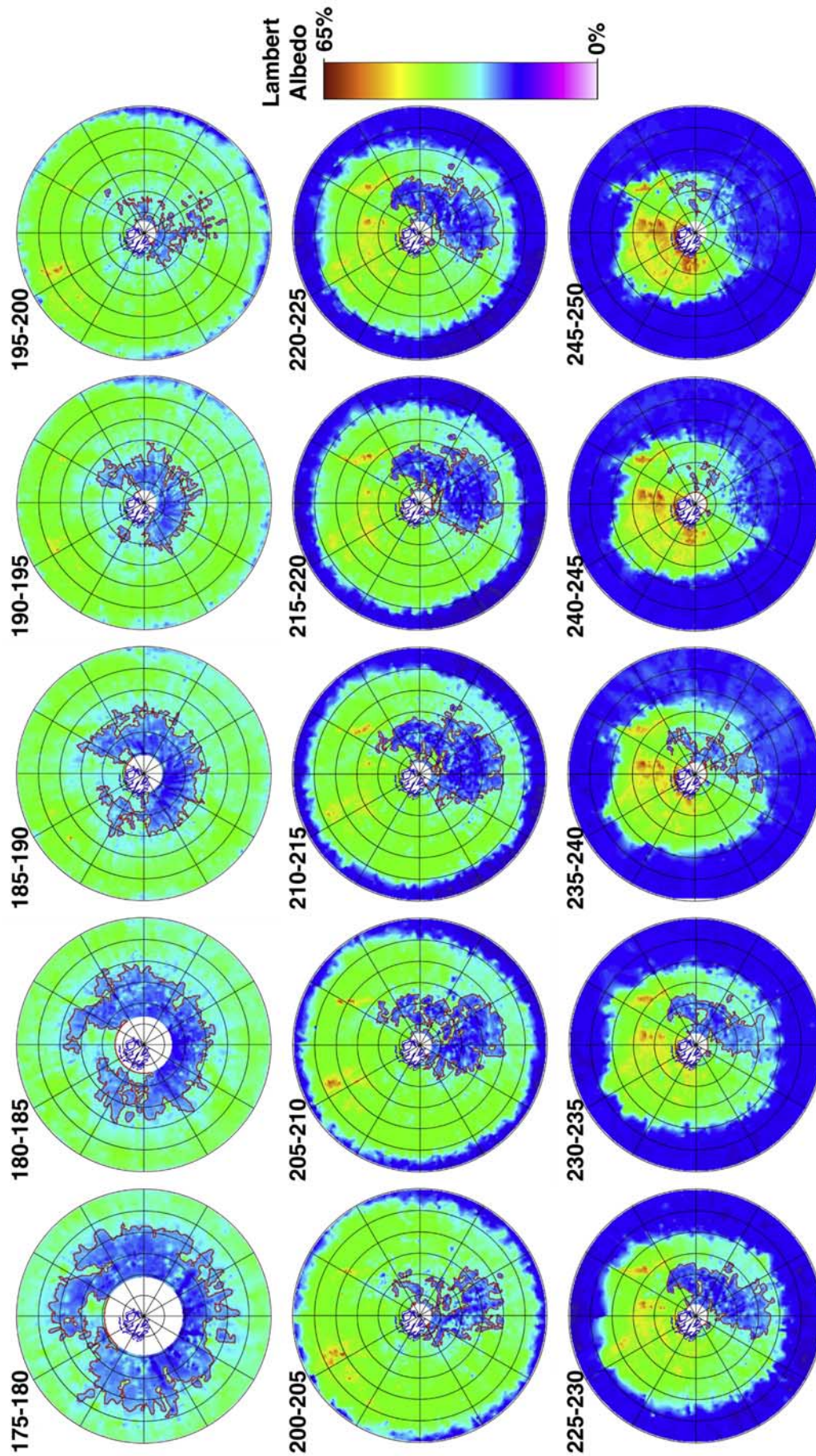


Figure 4. Evolution of the cryptic terrain as a function of season from the south pole to 60°S . Each image spans 5° of L_s from 180° to 250° . Shown here is TES Lambert albedo as a color gradient. We define the cryptic terrain to be areas with Lambert albedos < 0.38 and surface temperatures (from TES T_{20} equivalent) corresponding to solid CO_2 . The resulting “cryptic terrain” for each time period is outlined in red. Latitude and longitude lines are every 5° and 30° , respectively. White central circles represent areas of no data during that time period.

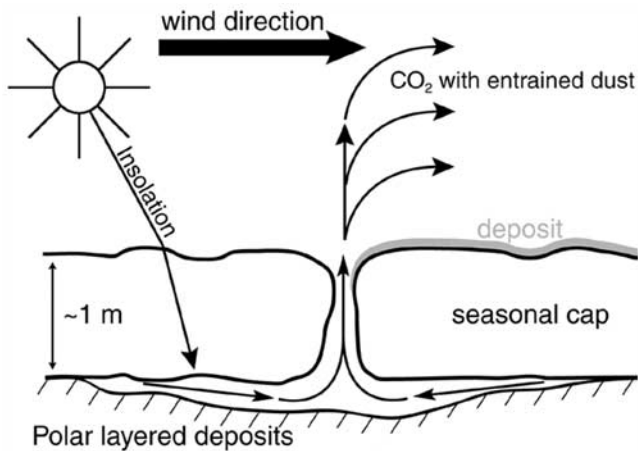


Figure 5. Schematic sketch of the CO₂ geyser hypothesis. South polar layered terrain is overlain by seasonal ice of ~1 m in thickness. Penetration of sunlight to the base of the seasonal deposit causes sublimation from the bottom, leading to a buildup of pressurized CO₂ gas. The gas eventually bursts out, entraining dust and leading to the dark fan-shaped deposits seen in Figure 6. Repeated outbursts from year to year erode the underlying polar layered deposits, leading to the development of spiders.

shrinks to a minimum at $L_s = 200^\circ$. At this point the cryptic region occupies only a small fraction of its initial extent and nearly disappears. The cryptic region then begins to expand in the direction of 150° – 300° W. Between $L_s = 205^\circ$ and $L_s = 230^\circ$ the cryptic region takes the form previously discussed by Kieffer *et al.* [2000]. After this period the cryptic region merges with the retreating edge of the seasonal cap and fades from view. The blank circle centered on the pole earlier in the season represents regions where no data were collected. We cannot state whether or not these regions exhibited cryptic behavior during the times when there were no data available.

[17] It can be seen from Figure 4 that some areas exhibit cryptic behavior for only part of the time that they are covered with CO₂ ice. Since we do not know when in the season individual spiders or spider regions formed, it is necessary to develop some form of aggregate definition of what constitutes the cryptic region. The most inclusive definition is that region which includes any area displaying cryptic behavior at any time during the defrosting season. However, much of this region only exhibits cryptic behavior at the very beginning of the southern spring. We show two aggregate cryptic regions in Figure 2a with the outline of the layered deposits [Kolb *et al.*, 2003] and spider distribution superposed. The smaller cryptic region is defined as including any location that exhibited cryptic behavior between $L_s = 190^\circ$ and the final sublimation of the seasonal cap. This smaller cryptic region is confined to the layered deposits and the floor of the Prometheus impact basin, while the more inclusive definition results in a cryptic region that includes all of the above and parts of the Dorsa Argentia and southern highland units. Figure 2a also shows the outlines of the areas within MOC images that contain spiders.

[18] It can be seen that all of the identified spiders, with very few exceptions (84° S, 20° W; 84° S, 320° W), fall within

regions defined by the more inclusive definition of cryptic terrain, and the majority fall within the more narrowly defined region. The exceptions noted fall within an area that is never described as cryptic using our criteria with the TES data. We believe this is due to a lack of data and that the surface in that location does exhibit cryptic behavior early in the season. Figure 4 shows the TES albedo values used to define the cryptic region. The first few subframes have a large white circle in the center where no data were acquired. This was presumably due to the very low light levels at that time of year. Since the albedo was not measured, we cannot state that this area is cryptic; however, on the basis of the distribution of cryptic terrain around it, is likely that this area was also exhibiting cryptic behavior during this time.

[19] Notably, all occurrences of spiders fall on areas historically mapped as polar layered deposits [Tanaka and Scott, 1987]. No instances are observed on the residual cap or in the surrounding cratered highlands. One group of spiders mapped at 82° S, 325° W is not included in the more recent definition of the polar layered deposits (this is the definition shown in Figure 2a) [Kolb *et al.*, 2003]. These spiders occur on a unit which is now defined as Amazonian mantled material and which is therefore superficially similar to the layered deposits, which is all that matters to these shallow landforms.

6. Discussion

[20] The conceptual model for the formation of spiders is illustrated in Figure 5. This model is based closely on those proposed for geysers on Neptune's moon Triton [Kirk *et al.*, 1990] and that extended to Mars by Kieffer [2000]. The model posits that transparent ice allows solar radiation to penetrate to the underlying surface. The heat absorbed by the ground provides the latent heat necessary to sublime CO₂ ice at the bottom of the seasonal ice cap. The trapped CO₂ gas will be at pressure and will exploit any weaknesses in the overlying ice in order to escape and vent into the atmosphere. When the gas pressure has forced a route to the surface, gas from the surrounding subice region will rush to it, generating grooves in weakly consolidated surface material. Some of this material will be lofted through the forced opening in the ice, forming an atmospheric plume. Material in this plume can be transported downwind before settling on the surface, forming fan-shaped deposits.

[21] Evidence for venting and its association with spider landforms can be seen in MOC NA imagery. An example of one such image is shown in Figure 6. Here one can see the coincidence of dark fan-shaped deposits and the underlying spiders. At this time the seasonal ice cover is thick and contiguous, and as such, the presence of wind-blown dust particles requires a mechanism for supply from beneath the ice. It is unlikely that this material is supplied externally from the atmosphere since it is strongly concentrated into fans that show a decreasing contrast with surrounding terrain (and hence thickness of deposit) with increasing distance from their vertices.

[22] Spiders do not occur everywhere that there is cryptic terrain; they are also confined (with only one exception) to the polar layered deposits. Thermal inertia studies indicate that the surface of the polar layered deposits is likely made

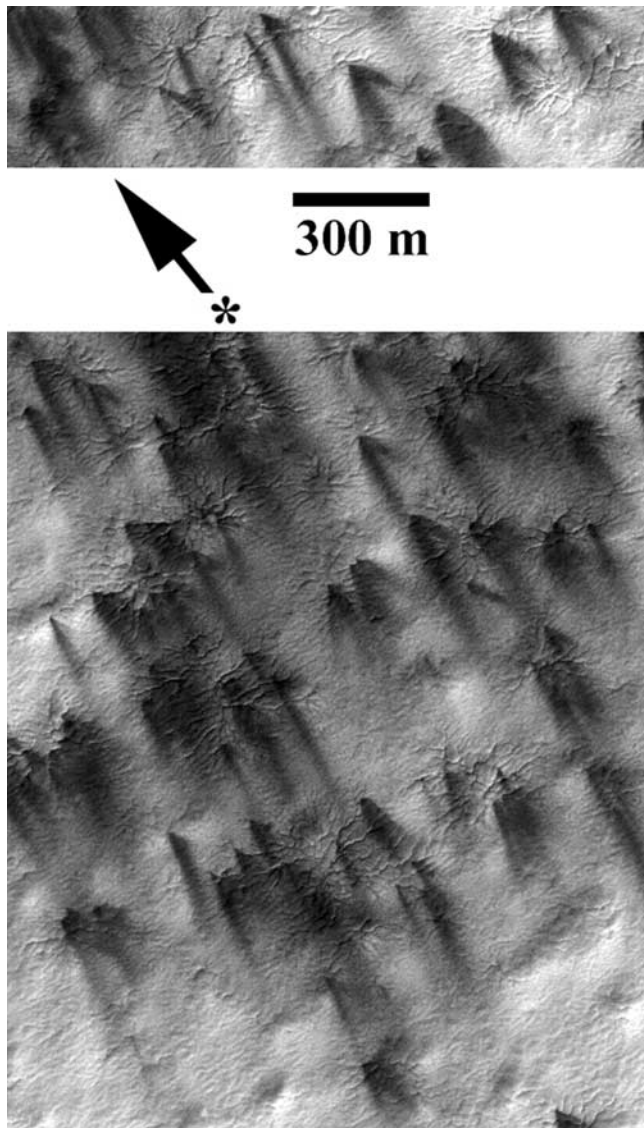


Figure 6. MOC NA image showing dark fans apparently emanating from the center of spider features. The image is M07/03150, taken at $L_s = 208^\circ$ and from 85.4°S , 257.1°W . The illumination direction and scale are as shown. The original image had a resolution of 2.8 m pixel^{-1} .

up of loosely consolidated material which is easily eroded [Vasavada *et al.*, 2000]. The same process of subice energy deposition and plume breakout is likely occurring on other units that exhibit cryptic behavior, such as the southern highlands on the floor of the Prometheus basin. However, the lack of a surface that is easily eroded limits the ability of these geysers to both erode spiders and entrain debris to form fan-shaped deposits.

[23] In order for the geyser hypothesis to work, there needs to be a pressure difference between sublimated CO₂ trapped beneath the seasonal ice and the atmosphere. It is easy to show that sublimation from the bottom of the seasonal cap generates substantial gas pressures. By virtue of the fact that the CO₂ is transparent, we know that it must be well consolidated with few scattering centers for visible radiation and hence likely characterized by the bulk density

of solid CO₂ ice. As such, we can estimate the pressure of the trapped gas by assuming that when the ice is sublimated, the volume will remain constant. This simple analysis results in a pressure of $>4 \times 10^7 \text{ Pa}$ (for a CO₂ ice density of 1600 kg m^{-3} , a gas constant of $187 \text{ J kg}^{-1} \text{ K}^{-1}$, and a temperature of 148 K). This is four orders of magnitude higher than the ice overburden pressure and five orders of magnitude higher than atmospheric pressure. Of course, this pressure will never be realized at the base of the seasonal cap as some fraction of the CO₂ gas will migrate through the underlying regolith. However, it is clear that sublimation of the base of the seasonal ice cap is more than capable of generating a substantial overpressure.

[24] The timescale for spider formation is largely unconstrained. However, it would seem that multiple years would be required to carve the channels. A comparison of imaging data from two separate years shows that the spider landforms are basically unchanged over these timescales (see Figure 7). This would imply that spiders form at the same locations from year to year. It is possible that the channels themselves lead to an increased likelihood of geyser formation, although the reasons for this are unclear.

7. Summary

[25] The theory of spider formation presented in this paper requires basal sublimation of the seasonal CO₂ ice cap by penetration of solar radiation through transparent ice to the underlying surface. We have shown that spiders only form within the cryptic terrain that is defined by the existence of transparent ice [Kieffer *et al.*, 2000]. The theory suggests that easily erodable surface material is necessary for the formation of the spider's grooves. We have further shown that spiders only form upon the south polar layered deposits, which are known to be mantled by poorly consolidated particulate material (with one exception on an equally mantled unit) based on thermal inertia measure-

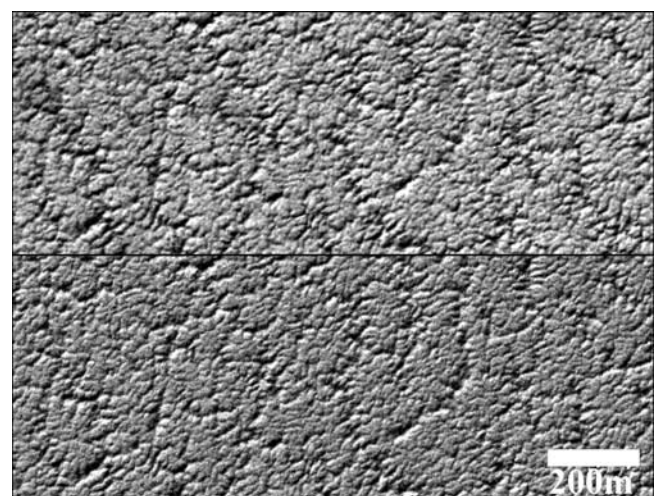


Figure 7. Comparison of spider landforms from one Martian year to the next at 87°S , 262°W . The top panel is a subframe of M11/03283 at $L_s = 287^\circ$; the bottom panel is a subframe of E14/01121 at $L_s = 343^\circ$. In both cases the illumination is from just left of top and north is directly to the right.

ments [Vasavada *et al.*, 2000]. An integral part of the spider-geyser hypothesis is the ejection of gas from the base of the seasonal ice cap. We have shown that spiders are closely associated with dark fan-shaped deposits, strongly suggesting that basal dust is being entrained within the geyser plumes. In this paper we have additionally described the seasonal evolution of spiders and of the cryptic terrain as observed by TES in its first mapping year.

[26] **Acknowledgments.** We wish to thank Hugh Kieffer and an anonymous referee for comments which substantially improved this paper. We also wish to thank Ken Tanaka and Eric Kolb for providing the outline of the southern residual cap and layered deposits. MIR and SB particularly wish to thank Hugh Kieffer for a never-ending stream of imaginative and creative nomenclature that substantially enhances the pleasure of working in this field. This work was supported by Caltech funds.

References

- Byrne, S., and B. C. Murray, North polar stratigraphy and the paleo-erg of Mars, *J. Geophys. Res.*, 107(E6), 5044, doi:10.1029/2001JE001615, 2002.
- Hess, S. L., R. M. Henry, and J. E. Tillman, The seasonal variation of atmospheric pressure on Mars as affected the south polar cap, *J. Geophys. Res.*, 84, 2923–2927, 1979.
- James, P. B., H. H. Kieffer, and D. A. Paige, The seasonal cycle of carbon dioxide on Mars, in *Mars*, edited by H. H. Kieffer *et al.*, pp. 934–968, Univ. of Ariz. Press, Tucson, Ariz., 1992.
- Kieffer, H. H., Annual punctuated CO₂ slab-ice and jets on Mars, paper presented at the 2nd International Conference on Mars Polar Science and Exploration, Univ. of Iceland, Reykjavik, 21–25 Aug. 2000.
- Kieffer, H. H., and T. N. Titus, TES mapping of Mars' north seasonal cap, *Icarus*, 154(1), 162–180, 2001.
- Kieffer, H. H., and A. P. Zent, Quasi-periodic climate change on Mars, in *Mars*, edited by H. H. Kieffer *et al.*, pp. 1180–1218, Univ. of Ariz. Press, Tucson, Ariz., 1992.
- Kieffer, H. H., B. M. Jakosky, and C. W. Snyder, The planet Mars: From antiquity to the present, in *Mars*, edited by H. H. Kieffer *et al.*, pp. 1–33, Univ. of Ariz. Press, Tucson, Ariz., 1992.
- Kieffer, H. H., T. N. Titus, K. F. Mullins, and P. R. Christensen, Mars south polar spring and summer behavior observed by TES: Seasonal cap evolution controlled by frost grain size, *J. Geophys. Res.*, 105, 9653–9699, 2000.
- Kirk, R. L., R. H. Brown, and L. A. Soderblom, Subsurface energy-storage and transport for solar-powered geysers on Triton, *Science*, 250, 424–429, 1990.
- Kolb, E. J., K. L. Tanaka, and J. A. Skinner, A new mapping approach for highland materials in the south polar region of Mars, *Lunar Planet. Sci. Conf.*, XXXIV, 2105–2108, 2003.
- Leighton, R. B., and B. C. Murray, Behavior of carbon dioxide and other volatiles on Mars, *Science*, 153, 136–144, 1966.
- Murray, B. C., M. Koutnik, S. Byrne, L. A. Soderblom, K. E. Herkenhoff, and K. L. Tanaka, Preliminary geological assessment of the northern edge of Ultimi lobe: Mars south polar layered deposits, *Icarus*, 154(1), 80–97, 2001.
- Tanaka, K. L., and D. H. Scott, Geologic map of the polar regions of Mars, Inv. Series Map I-1802-C, scale 1:15,000,000, U. S. Geol. Surv., Washington, D. C., 1987.
- Vasavada, A. R., J.-P. Williams, D. A. Paige, K. E. Herkenhoff, N. T. Bridges, R. Greeley, B. C. Murray, D. S. Bass, and K. S. McBride, Surface properties of Mars' polar layered deposits and polar landing sites, *J. Geophys. Res.*, 105, 6961–6969, 2000.

S. Byrne, S. Piqueux, and M. I. Richardson, Division of Geological and Planetary Sciences, California Institute of Technology, MS 150-21, Pasadena, CA 91125, USA. (shane@gps.caltech.edu; sylvain.piqueux@free.fr; mir@gps.caltech.edu)